

Metamaterial of rod pairs standing on gold plate and its negative refraction property in the far-infrared frequency regime

F. M. Wang,¹ H. Liu,^{1,2} T. Li,¹ Z. G. Dong,¹ S. N. Zhu,^{1,*} and X. Zhang²

¹*Department of Physics, National Laboratory of Solid State Microstructures, Nanjing University, Nanjing 210093, People's Republic of China*

²*5130 Etcheverry Hall, Nanoscale Science and Engineering Center, University of California, Berkeley, California 94720-1740, USA*

(Received 6 June 2006; published 10 January 2007)

A new kind of metamaterial, an array of periodic gold rod pairs standing on gold substrate, is introduced in this paper. A commercial electromagnetic mode solver, the High-Frequency Structure Simulator, is employed to explore the propagation property of electromagnetic waves in this system. When an *S*-polarized electromagnetic (EM) wave propagates along the substrate surface, strong magnetic resonance is produced in the far-infrared regime. Based on the simulated *S* parameters, effective refractive index is retrieved and negative value is obtained over the wavelength range from 49.2 μm to 66.7 μm . A wedge made of this metamaterial with an inclined angle 26.6° is designed. An observable negative refraction behavior of EM wave is attained in this structure at wavelength 61.2 μm . The refractive index is calculated by Snell's law and it is consistent with the retrieved results quite well. This provides direct evidence for the negative refraction property.

DOI: 10.1103/PhysRevE.75.016604

PACS number(s): 41.20.Jb, 78.20.Ci, 73.20.Mf

In 1968, a novel material, called left-handed media (LHM), was first theoretically discussed by Veselago [1]. With simultaneously negative permittivity ϵ and permeability μ , LHM exhibits an astonishing negative refraction property. In recent years, Pendry proposed a kind of composite effective media, consisting of split-ring resonators (SRRs) and continuous wires, which can behave like LHM [2,3]. Initiated by the first experimental materialization of Pendry's idea in microwave regime [4], more and more studies have been focused on this kind of metamaterial [5–9], particularly in the higher frequency range. Until now, some new structures have already been invented to present magnetic resonance at infrared and visible light [10–19]. Among them, cut-wire pairing is a very simple system [18,19], possessing negative permittivity ϵ and permeability μ naturally, which leads to a negative index without using conventional SRRs and wires. In another recent paper, Shalaev *et al.* proved experimentally that such a system is able to realize negative refractivity at the optical communication frequency [20].

However, in Shalaev's experiment setup, only one layer of cut-wire pairs was laid on a glass substrate and electromagnetic (EM) wave propagated perpendicularly to the substrate plane. The thickness of this effective media was far smaller than the incident wavelength, and the refractive index of the structure was only retrieved from the phase and amplitude of the wave's transmission and reflection. No direct negative refraction analysis using Snell's law was performed as Shelby *et al.* achieved in their microwave measurement [5].

In this work, we propose a new configuration in which every unit cell consists of two parallel rods as well, but they stand on a metal substrate, as shown in Fig. 1. These unit cells are repeated periodically in the substrate plane. Different from Shalaev's scheme, we make the EM wave propagate along the substrate surface. In this system, two standing

parallel metal rods can still produce magnetic resonance as Shalaev achieved. Besides, stronger magnetic resonance can take place in the pairs of rods due to metal substrate replacing a glass one. Correspondingly, a small, imaginary part of n in the negative-permeability band results in low loss in the transmission process. Additionally, the most important advantage of this arrangement is that the propagating length of light in the effective media can be much longer than the wavelength. The negative refraction property can be proved directly based on Snell's law. In the following text, we construct a wedge shape of the metamaterial to demonstrate the refraction behavior of the structure by numerical simulation. The refractive indices obtained by Snell's Law are consistent with the results retrieved from the *S* parameters, providing a strong evidence for the negative refraction property.

For the structure depicted in Fig. 1, the gold rod pair combined with the metal plate form an equivalent "U"-shaped LC circuit. The U shape part works as the inductor L , and the gap between the two rod pairs acts as a capacitor C . For an EM wave incident with the electric field polarized along the rods and the magnetic field perpendicular to the rod pair, magnetic resonances can be generated at certain frequencies. At the resonance frequency, conduction current

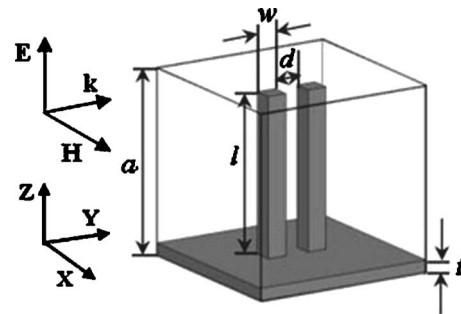


FIG. 1. Schematic of a cubic unit cell of the metamaterial used in our simulations with $a=15 \mu\text{m}$, $w=1.6 \mu\text{m}$, $l=13 \mu\text{m}$, $d=2 \mu\text{m}$ and $t=1 \mu\text{m}$.

*Author to whom correspondence should be addressed. Email address: zhun@nju.edu.cn

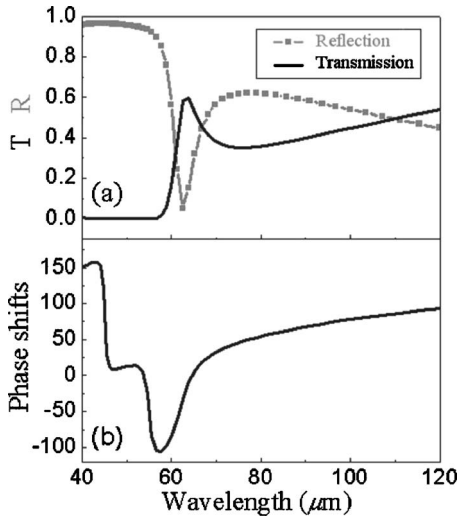


FIG. 2. (a) Simulated transmission T (black curve) and reflection R (gray curve with closed square) spectra for a unit cell. (b) Phase shifts for transmission of EM wave through a unit cell.

is induced in the U shape and displacement current is produced in the gap, respectively. This circulating current around the U-shaped loop leads to a magnetic moment parallel to the metal plate surface, counteracting the change of external magnetic field, which results in negative permeability.

To study the EM response of the proposed structure, we perform a set of finite element numerical method (FEM) calculations using a commercial software package HIGH-FREQUENCY STRUCTURE SIMULATOR (HFSS), a commercial electromagnetic mode solver. The property of metal material (gold) is treated as a dispersive medium following the Drude dispersion model [$\epsilon = 1 - \omega_p^2 / (\omega^2 + i\omega\gamma)$], with its plasma frequency of gold $\omega_p = 1.37 \times 10^{16} \text{ s}^{-1}$ and scattering frequency $\gamma = 4.08 \times 10^{13} \text{ s}^{-1}$.

The unit cell is put in a waveguide with the size shown as the frame in Fig. 1. Polarized EM wave propagates in the Y direction, with magnetic field in the X direction (perpendicular to the rod pair plane) and electric field in the Z direction (along the rod). The calculation results for transmission (black curve) and reflection (gray curve with closed square) spectra is presented in Fig. 2(a). There is a transmission peak around a wavelength 61.2 μm . In order to prove that strong magnetic resonance happens at this wavelength, we calculate the distribution of induced current inside the structure at

61.2 μm and another nonresonance wavelength 115.4 μm , which are compared in Fig. 3. The result for the resonance case is shown in Fig. 3(a), in which much larger current (ten times greater than the nonresonance case) is induced inside the structure. If we check the direction of the current in the rods, it is obviously seen that the current forms a loop encircling the U-shaped circuit, producing a substantial magnetic moment. For the nonresonance case at 115.4 μm , as shown in Fig. 3(b), the currents flowing in two rods are of the same direction and they cannot form a loop, which does not produce any significant magnetic moment. The above comparison demonstrates that the transmission peak in Fig. 2(a) originates from magnetic resonance in the rods and metal plate system. Note that the currents in the metal substrate surface also contribute to the total current oscillations, which results in a stronger magnetic resonance compared with just two metal rods on glass substrate (Shalaev's design).

From the above simulation data, the phase shift of the EM wave through one unit cell is calculated according to the method described in Ref. [20]. The result is given in Fig. 2(b). Here, the phase shift is defined as the difference of phase change between one unit cell (φ_s) and a reference layer of air (φ_r) with the same propagation length: $\delta\varphi = \varphi_s - \varphi_r$. In the calculated curve, there is a big trough around the magnetic resonance wavelength. Furthermore, part of the curve is below zero and indicates that left-handed (LH) behavior exists in this region.

The effective media model can be applied to retrieve permittivity ϵ , permeability μ , and the refractive index n , using the S -parameter retrieval methods described in Refs. [21–23]. Basically, the effective parameters are dependent on the polarization of incident wave. In all following discussions, the propagation of EM wave is supposed to be parallel to the substrate surface. For P polarization (magnetic field is perpendicular to the substrate), the magnetic field vector has no component penetrate the U-shaped circuit and there is no magnetic response excited. For S polarization (electric field is perpendicular to the substrate), the rod pairs are expected to respond magnetically when the magnetic field is perpendicular to the U-shaped circuit and to exhibit no magnetic response when the magnetic field is parallel to the U-shaped circuit. While the incident wave propagates at a certain non-zero angle to the U-shaped circuit, the magnetic field vector has a component normal to the resonance circuit. The magnetic resonance will still occur around the wavelength of 61.2 μm , but resonant strength becomes weaker. Here, we investigate the case that the magnetic field of the incident

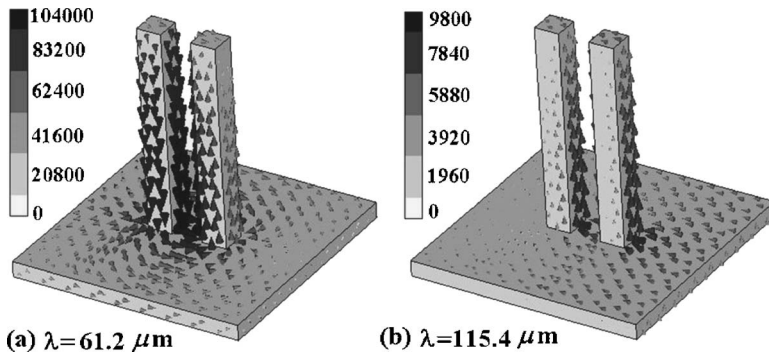


FIG. 3. Distribution of induced current in the rod pair and metal plate at a wavelength of (a) 61.2 μm and (b) 115.4 μm .

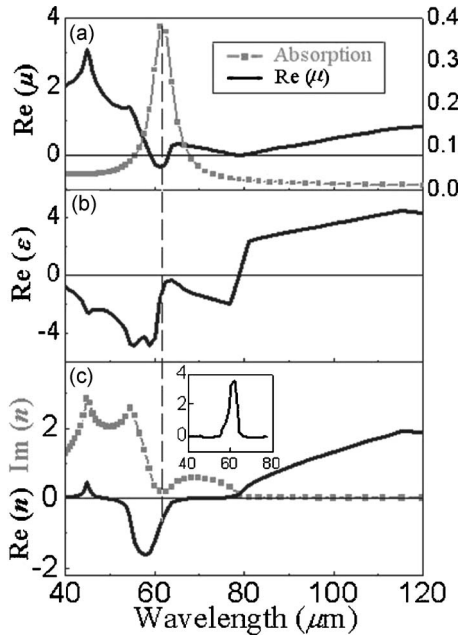


FIG. 4. The retrieved results of effective coefficients: (a) real part of permeability $\text{Re}(\mu)$ (black curve); (b) real part of permittivity $\text{Re}(\epsilon)$; (c) real (black curve) and imaginary (gray curve with closed square) parts of the refractive index; the absolute value of ratio of $\text{Re}(n)/\text{Im}(n)$ (inset). The gray curve in (a) is represented for absorption spectra calculated from transmission and reflection data.

wave is perpendicular to the U-shaped circuit, which exhibits the strongest response. The above S -parameter data for one unit cell are used in the retrieval procedure. The effective permeability is obtained as in Fig. 4(a) (black curve). Due to the strong magnetic resonance in the U-shaped loops, negative permeability is obtained over a narrow range of wavelengths, from $59.1 \mu\text{m}$ to $63.2 \mu\text{m}$. The real part of μ shows a small trough around $61.2 \mu\text{m}$, indicating the existence of the magnetic activity in this wavelength range. The absorption curve (gray curve with closed square) is also provided in Fig. 4(a). We note that the maximum absorption occurs at the strongest magnetic resonance wavelength [$\text{Re}(\mu)_{\min} = -0.33$ at $61.2 \mu\text{m}$]. The location of the LH transmission peak takes place slightly below the absorption peak in the negative μ region, because the strong magnetic resonance prevents the maximum transmission and the minimum permeability appearing at the same position. Negative permittivity is obtained over a wider range of wavelengths from $40 \mu\text{m}$ to $76.9 \mu\text{m}$ [see Fig. 4(b)], which covers the range of the negative permeability. At last, the effective refractive index is calculated as shown in Fig. 4(c), taking a negative-values range from $49.2 \mu\text{m}$ to $66.7 \mu\text{m}$. The result is in good agreement with the resonance region of the phase shifts in Fig. 2(b). Though there exists only a narrow wavelength range in which effective permeability and permittivity are negative simultaneously, a wide negative $\text{Re}(n)$ range is still achieved as the condition $\epsilon_1\mu_2 + \epsilon_2\mu_1 < 0$ is satisfied [24], where $\epsilon = \epsilon_1 + i\epsilon_2$ and $\mu = \mu_1 + i\mu_2$. In our simulation results, the sign of $\epsilon_1\mu_2 + \epsilon_2\mu_1$ is well consistent with that of $\text{Re}(n)$. An important LHM quality, the absolute value of the ratio

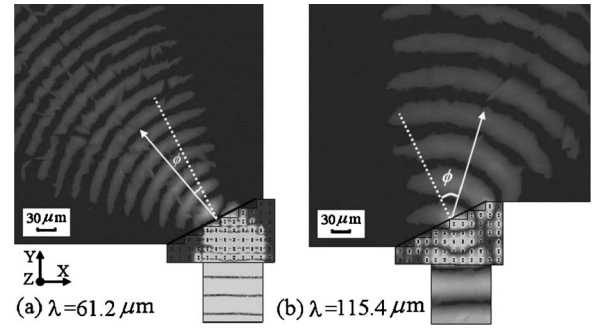


FIG. 5. The magnitude distribution of electric field for the refraction in a wedge-shaped structure at wavelengths of (a) $61.2 \mu\text{m}$ and (b) $115.4 \mu\text{m}$.

n_1/n_2 , is plotted in Fig. 4(c), inset, where n_1 and n_2 are the real and imaginary parts of the refractive index. With $-n_1 > n_2$ over the range of wavelengths from $57.7 \mu\text{m}$ to $62.5 \mu\text{m}$, high transmission with low loss is achieved.

In order to verify the above negative refractive index value by Snell's law and give a direct image of the negative-refraction behavior of the EM wave, a two-dimensional wedge with an inclined angle of 26.6° is designed for simulation, as shown in Fig. 5. The refraction interface of the wedge actually has a staircase pattern, which is designed similar to the actual samples used in experiments [5]. Since the wavelengths ($\sim 60 \mu\text{m}$) are much larger than the unit cell size ($15 \mu\text{m}$), the wedge can be treated as an effective homogeneous medium for incident wave. For the wedge of 26.6° , 12 unit cells ($180 \mu\text{m}$) are arrayed along the X axis and 7 unit cells ($105 \mu\text{m}$) along the Y axis, shown in Fig. 5. The wedge is positioned between two electrically conducting plates to form a two-dimensional waveguide. The spacing between the two electrically conducting plates is $15 \mu\text{m}$ (thickness of one unit cell). An EM wave is guided by a rectangular channel and shined on the first interface of the wedge normally. After it gets through the wedge effective media, the wave will undergo refraction at the second interface. Note that such two-dimensional composite structures exhibit LHM behavior only for the S -polarization wave. Hence, the polarization of the wave guided by the channel is defined as with magnetic field in the X direction and electric field in the Z direction. Between the two electrically conducting plates, the EM wave can keep its polarization and propagate through the whole system.

Figure 5 illustrates the magnitude distribution of the electric field at the midplane between two electrically conducting plates at the incident wavelength of $61.2 \mu\text{m}$ and $115.4 \mu\text{m}$. In the LH range from $49.2 \mu\text{m}$ to $66.7 \mu\text{m}$, the polarized EM wave is refracted negatively due to the negative nature of $\text{Re}(n)$. The surface normal is shown by the dotted line and the solid arrow indicates the transmission direction of the refracted wave in the figure. Figure 5(a) shows the typical electric field distribution in this range at $61.2 \mu\text{m}$. We see that the refracted wave and incident wave are clearly in the same side with respect to the surface normal, which can be justified as negative refraction. In Fig. 5(b), for an incident wave at $115.4 \mu\text{m}$, as the wavelength is out of the negative

range, the EM wave is refracted positively as we expected. With the same incident angle 26.6° , the refracted angles (ϕ) in Figs. 5(a) and 5(b) are determined as $-20^\circ \pm 1^\circ$, $55^\circ \pm 3^\circ$ with respect to the normal direction of output interface, respectively. Based on Snell's law, the effective refraction indices are calculated as -0.76 ± 0.04 and 1.83 ± 0.07 . The retrieved refractive indices from the S parameters at these two wavelengths are -0.77 and 1.91 , respectively. The results obtained from these two different methods are consistent with each other quite well. The deviation of the right-handed refracted angle is a little bigger. This is because the divergence angle of the refraction wave at $115.4 \mu\text{m}$ is too large, which brings more error to set the refraction angle. In addition, we also investigate the refraction behavior with an alternative inclined angle of the wedge, 18.4° . With the two same incident wavelengths, $61.2 \mu\text{m}$ and $115.4 \mu\text{m}$, the direction of refraction does not change for these two cases. Negative refraction is still obtained at $61.2 \mu\text{m}$, with a refraction angle of about -14° , which still conforms to Snell's law.

In conclusion, an array of periodic gold rod pairs standing on gold substrate has been reported in this paper. Numerical simulations are carried out to investigate the negative refraction property of this structure. When an S -polarized EM wave propagates along the substrate surface, strong magnetic resonance is found around wavelengths of $61.2 \mu\text{m}$. An effective refraction index is retrieved from the simulated S parameters, and a negative value is obtained over the wavelength range from $49.2 \mu\text{m}$ to $66.7 \mu\text{m}$. In a wedge-shaped structure composed from this metamaterial, the negative refraction behavior is obtained at $61.2 \mu\text{m}$ wavelength. This provides direct evidence for the negative refraction property.

This work was supported by the State Key Program for Basic Research of China (No. 2004CB619003), the National Key Projects for Basic Researches of China (No. 2006CB0L1004), and the National Natural Science Foundations of China under Contracts No. 10534020, No. 60578034, and No. 10604029.

-
- [1] V. G. Veselago, *Sov. Phys. Usp.* **10**, 509 (1968).
 [2] J. B. Pendry, A. J. Holden, W. J. Stewart, and I. Youngs, *Phys. Rev. Lett.* **76**, 4773 (1996).
 [3] J. B. Pendry, A. J. Holden, D. J. Robbins, and W. J. Stewart, *IEEE Trans. Microwave Theory Tech.* **47**, 2075 (1999).
 [4] D. R. Smith, W. J. Padilla, D. C. Vier, S. C. Nemat-Nasser, and S. Schultz, *Phys. Rev. Lett.* **84**, 4184 (2000).
 [5] R. A. Shelby, D. R. Smith, and S. Schultz, *Science* **292**, 77 (2001).
 [6] C. G. Parazzoli, R. B. Gregor, K. Li, B. E. C. Koltenbah, and M. Tanielian, *Phys. Rev. Lett.* **90**, 107401 (2003).
 [7] A. A. Houck, J. B. Brock, and I. L. Chuang, *Phys. Rev. Lett.* **90**, 137401 (2003).
 [8] K. Aydin, K. Guven, C. M. Soukoulis, and E. Ozbay, *Appl. Phys. Lett.* **86**, 124102 (2005).
 [9] Z. G. Dong, S. N. Zhu, H. Liu, J. Zhu, and W. Cao, *Phys. Rev. E* **72**, 016607 (2005).
 [10] T. J. Yen, W. J. Padilla, N. Fang, D. C. Vier, D. R. Smith, J. B. Pendry, D. N. Basov, and X. Zhang, *Science* **303**, 1494 (2004).
 [11] S. Linden, C. Enkrich, M. Wegener, J. Zhou, Th. Koschny, and C. M. Soukoulis, *Science* **306**, 1351 (2004).
 [12] S. Zhang, W. Fan, B. K. Minhas, A. Frauenglass, K. J. Malloy, and S. R. J. Brueck, *Phys. Rev. Lett.* **94**, 037402 (2005).
 [13] N. Katsarakis, G. Konstantinidis, A. Kostopoulos, R. S. Penci, T. F. Gundogdu, M. Kafesaki, E. N. Economou, T. Koschny, and C. M. Soukoulis, *Opt. Lett.* **30**, 1348 (2005).
 [14] A. Ishikawa, T. Tanaka, and S. Kawata, *Phys. Rev. Lett.* **95**, 237401 (2005).
 [15] C. Enkrich, M. Wegener, S. Linden, S. Burger, L. Zschiedrich, F. Schmidt, J. F. Zhou, Th. Koschny, and C. M. Soukoulis, *Phys. Rev. Lett.* **95**, 203901 (2005).
 [16] G. Dolling, C. Enkrich, M. Wegener, J. F. Zhou, C. M. Soukoulis, and S. Linden, *Opt. Lett.* **30**, 3198 (2005).
 [17] A. N. Grigorenko, A. K. Geim, H. F. Gleeson, Y. Zhang, A. A. Firsov, I. Y. Khrushchev, and J. Petrovic, *Nature (London)* **438**, 335 (2005).
 [18] V. A. Podolskiy, A. K. Sarychev, and V. M. Shalaev, *Opt. Express* **11**, 735 (2003).
 [19] L. V. Panina, A. N. Grigorenko, and D. P. Makhnovskiy, *Phys. Rev. B* **66**, 155411 (2002).
 [20] V. M. Shalaev, W. Cai, U. K. Chettiar, H. K. Yuan, A. K. Sarychev, V. P. Drachev, and A. V. Kildishev, *Opt. Lett.* **30**, 3356 (2005).
 [21] D. R. Smith, S. Schultz, P. Markoš, and C. M. Soukoulis, *Phys. Rev. B* **65**, 195104 (2002).
 [22] X. Chen, T. M. Grzegorzczuk, B. I. Wu, J. Pacheco, Jr., and J. A. Kong, *Phys. Rev. E* **70**, 016608 (2004).
 [23] D. R. Smith, D. C. Vier, Th. Koschny, and C. M. Soukoulis, *Phys. Rev. E* **71**, 036617 (2005).
 [24] S. Zhang, W. Fan, N. C. Panoiu, K. J. Malloy, R. M. Osgood, and S. R. J. Brueck, *Phys. Rev. Lett.* **95**, 137404 (2005).